

2) 学会発表

-国内学会-

第 35 回日本小児遺伝学会学術集会
2012.4.18-19 久留米大学筑水会館 (久留米市)

複数弁置換術および冠動脈拡大を伴い成人期まで経過観察し得ている Shprintzen-Goldberg 症候群の一例. 家村素史、渡邊順子、高瀬隆太、吉本裕良、工藤嘉公、芳野 信、松石豊次郎、吉田晶子、森崎裕子、森崎隆幸、須田憲治

第 115 回日本小児科学会 2012.4.20-22 福岡国際会議場 (福岡市)

骨髄移植を受けた I-cell 病の長期予後. 渡邊順子、矢部晋正、加藤俊一、大友孝信、酒井則夫、賀佐伸省、松石豊次郎、芳野 信

高度肺気腫に対し肺容量減少術が著効した FLNA1 遺伝子変異を持つ女兒の術語経過報告.

十亀由喜子、岡松由記、木村光一、渡邊順子、芳野 信、松石豊次郎:

SNP に基づくハプロタイプ解析による差異 OTC アレルの特定. 芳野 信、原田なをみ、沼田早苗、渡邊順子、神田芳郎、澤田 智、岡野善

Hunter 症候群患児に対する Idursulfatase 補充は心室中隔、左室後

壁肥厚を改善する.

高瀬隆太、大平智子、渡邊順子、須田憲治、松石豊次郎、芳野 信

Zellweger 症候群の点状石灰化の形態は鑑別診断上、価値がある. 芳野裕子、牛嶋規久美、下村 豪、松岡尚久、岡田純一郎、久野 正、浦部大策、芳野 信、下澤伸行

第 57 回日本人類遺伝学会 2012.10.24-27 京王プラザホテル (東京)

Perlman 症候群における *DIS3L2* のエクソン 9 の欠失は LINE-1 間の非相同組換えによって生じる. 東元 健、前田寿幸、八木ひとみ、岡田純一郎、佐々木健作、吉浦孝一郎、渡邊順子、副島英伸

22q11.2 欠失症候群の 2 家系の経験 Experience with 2 families carrying 22q11.2 Deletion Syndrome. 原田なをみ、沼田早苗、前野泰樹、須田憲治、芳野 信、松石豊次郎¹、橋本 隆、渡邊順子

第 54 回日本先天代謝異常学会 2012.11.15-17 じゅうろくプラザ (岐阜市)

Ornithine transcarbamylase(OTC)欠損症に潜在する凝固異常. 井原健二、吉野 信、保科隆之、原田なをみ、石井加奈子、長谷川有紀、渡邊順子、山口

清次、原 寿郎：

膝蓋骨の異常石灰化を契機に Zellweger 症候群の診断に至った一例。芳野裕子、牛嶋規久美、下村 豪、松岡尚久、岡田純一郎、久野 正、浦部大策、渡邊順子、芳野 信、下澤伸行

Two cases of NICCD diagnosed by urine organic acids based newborn screening. Yoriko Watanabe, Mina Furukawa, Kyoko Tashiro, Kumiko Aoki, Takahiro Inokuchi, Yoshitaka Seki, Tadahiro Yanagi, Tatsuki Mizuochi, Makoto Yoshino, Toyojiro Matsuishi

第 470 回日本小児科学会福岡地方会例会

2012.6.9 福大メディカルホール(福岡市)

乳糖除去 MCT ミルク(ML-3)を用いた NICCD の 1 例。古川実奈，水落建輝，横地 賢興，柳 忠宏，関 祥孝，渡邊順子，松石豊次郎、早坂 清、呉 繁夫

-国際学会-

Annual Symposium of the Society for the Study of Inborn Errors of Metabolism 2012.8.30-9.2 (Birmingham)

Two cases of neonatal onset type II

citrullinemia diagnosed by urine organic acids based newborn screening. Watanabe Y, Tashiro K, Aoki K, Seki Y, Yanagi T, Okada J, Mizuochi T, Inokuchi T, Yoshino M, Matsuishi T.

The American Society of Human Genetics, International Congress of Human Genetics, 62nd Annual Meeting Montreal, Canada, November 6-10, 2012

Two cases of neonatal onset type II citrullinemia diagnosed by urine organic acids based newborn screening. Watanabe Y, Tashiro K, Aoki K, Inokuchi T, Seki Y, Yanagi T, Mizuochi T, Yoshino M, Matsuishi T.

H. 知的財産権の出願・登録状況（予定を含む。）

1. 特許取得

なし

2. 実用新案登録

なし

3. その他

なし

厚生労働科学研究費補助金（難治性疾患克服研究事業）

平成24年度分担研究報告書

研究課題：地域蓄積・収集した希少疾患の系統的原因究明

分担研究項目：臨床診断、遺伝カウンセリング

分担研究者

園田 徹（九州保健福祉大学保健科学部作業療法学科・教授）

研究要旨

本研究の目的は地域蓄積・収集した希少疾患の系統的原因究明であり、そのための各症例の臨床診断、遺伝カウンセリングを担当した。地域蓄積する疾患とそれらの患者の試料収集を目指した。

A. 研究目的

地域蓄積する疾患とそれらの患者の試料収集を目的とした。

部運営委員会委員として、遺伝相談についての助言をしたり、月1回の症例検討会に出席したりした。

B. 研究方法

宮崎県内の主な新生児施設（宮崎大学医学部附属病院、県立宮崎病院、県立延岡病院、宮崎県医師会病院など）で先天異常の児が出生した場合、連絡が入り、診察に出かけた。宮崎大学医学部附属病院の遺伝カウンセリング

C. 研究結果

遠位関節拘縮症候群や10p-症候群などを経験したが、新しい奇形症候群の発見や地域蓄積する疾患の発見はなかった。

D. 考察

なかなか、症例の集積が難しい。

E. 結論

新しい奇形症候群や地域蓄積する疾

患の発見に努めたが、その目的を十分果たすことができなかった。

——達成度について——

今後はもっと研究全体に貢献できるようにしたい。

F. 健康危険情報

なし

G. 研究発表

1) 論文発表

1. Ikewaki N, Sonoda T, Nakamura M, Ishizuki T, Higuchi G, Sugimoto S. Action of *Taimatsu* fermented rice germ solution oh human immune

responses. *J of Kyushu Univ of Health and Welfare* 2013 Mar;14: 177-182.

H. 知的財産権の出願・登録状況（予定を含む。）

1. 特許得取得

なし

2. 実用新案登録

なし

3. その他

なし

III. 研究成果の刊行に関する一覧表

研究成果の刊行に関する一覧表

書籍

Kaname T, Yanagi K, Maehara H. Osteosarcoma and midkine. '*Midkine: From embryogenesis to pathogenesis and medication*' Ergüven M, Billir A, Muramatsu T. Eds. Springer, New York, pp313-319, 2012.

雑誌

発表者氏名	論文タイトル名	発表誌名	巻号	ページ	出版年
Nakazawa Y, Sasaki K, Mitsutake N, Matsuse M, Shimada M, Nardo T, Takahashi Y, Ohyama K, Ito K, Mishima H, Nomura M, Kinoshita A, Ono S, Takenaka K, Masuyama R, Kudo T, Slor H, Utani A, Tateishi S, Yamashita S, Stefanini M, Lehmann AR, Yoshiura KI, Ogi T.	Mutations in UVSSA cause UV-sensitive syndrome and impair RNA polymerase II processing in transcription-coupled nucleotide-excision repair.	<i>Nature Genetics</i>	44(5)	586-592	2012
Matsuse M, Sasaki K, Nishihara E, Minami S, Hayashida C, Kondo H, Suzuki K, Saenko V, Yoshiura K, Mitsutake N, Yamashita S.	Copy number alteration and uniparental disomy analysis categorizes Japanese papillary thyroid carcinomas into distinct groups.	<i>PLoS One</i>	74(4)	e36063	2012
Arai J, Tsuchiya T, Oikawa M, Mochinaga K, Hayashi T, Yoshiura KI, Tsukamoto K, Yamasaki N, Matsumoto K, Miyazaki T, Nagayasu T.	Clinical and molecular analysis of synchronous double lung cancers.	<i>Lung Cancer</i>	77(2):	281-287	2012

Ono S, Yoshiura K, Kinoshita A, Kikuchi T, Nakane Y, Kato N, Sadamatsu M, Konishi T, Nagamitsu S, Matsuura M, Yasuda A, Komine M, Kanai K, Inoue T, Osamura T, Saito K, Hirose S, Koide H, Tomita H, Ozawa H, Niikawa N, Kurotaki N.	Mutations in PRRT2 responsible for paroxysmal kinesigenic dyskinesias also cause benign familial infantile convulsions.	<i>J Hum Genet</i>	57(5):	338-341	2012
Mishima H, Aerts J, Katayama T, Bonnal RJ, Yoshiura K.	The Ruby UCSC API: accessing the UCSC genome database using Ruby.	<i>BMC Bioinformatics</i>	13	240	2012
Hikida M, Tsuda M, Watanabe A, Kinoshita A, Akita S, Hirano A, Uchiyama T, Yoshiura K.	No evidence of association between 8q24 and susceptibility to nonsyndromic cleft lip with or without palate in Japanese population.	<i>Cleft Palate Craniofac J</i>	49(6)	714-717	2012
Kawakami A, Migita K, Ida H, Yoshiura K, Arima K, Eguchi K.	[109th Scientific Meeting of the Japanese Society of Internal Medicine: educational lecture: 14. Autoinflammatory syndrome].	<i>Nihon Naika Gakkai Zasshi</i>	101(9)	2733-2739,	2012
Ogi T, Walker S, Stiff T, Hobson E, Limsirichaikul S, Carpenter G, Prescott K, Suri M, Byrd P, Matsuse M, Mitsutake N, Nakazawa Y, Vasudevan P, Barrow M, Stewart G, Taylor M, O'Driscoll M, and Jeggo P.	Identification of the first ATRIP-deficient patient and novel mutations in ATR define a clinical spectrum for ATR-ATRIP Seckel syndrome.	<i>PLoS Genetics</i>	8	e1002945	2012

Kashiyama K, Nakazawa Y, Pilz D, Guo C, Shimada M, Sasaki K, Fawcett H, Wing J, Lewin S, Carr L, Yoshiura K, Utani A, Hirano A, Yamashita S, Greenblatt D, Nardo T, Stefanini M, McGibbon D, Sarkany R, Fassihi H, Takahashi Y, Nagayama Y, Mitsutake N, Lehmann AR, and Ogi T.	Malfunction of the ERCC1/XPF endonuclease results in diverse clinical manifestations and causes three nucleotide excision-repair-deficient disorders, Cockayne Syndrome, xeroderma pigmentosum and Fanconi Anemia.	<i>American Journal of Human Genetics</i>	In press		2013
Suzumori N, Kaname T, Muramatsu Y, Yanagi K, Kumagai K, Mizuno S, Naritomi K, Saitho S, Sugiura M.	Prenatal diagnosis of X-linked recessive Lenz microphthalmia syndrome.	<i>J Obstetr Gynaecol Res</i>	In press		2013
Altıncık A, Kaname T, Demir K, Böber E.	A novel mutation in a mother and a son with Aarskog-Scott syndrome.	<i>J Pediatr Endocrinol Metab,</i>	26(3-4)	385-388	2013
Kosho T, Okamoto N, Ohashi H, Tsurusaki Y, Imai Y, Hibi-Ko Y, Kawame H, Homma T, Tanabe S, Kato M, Hiraki Y, Yamagata T, Yano S, Sakazume S, Ishii T, Nagai T, Ohta T, Niikawa N, Mizuno S, Kaname T, Naritomi K, Narumi Y, Wakui K, Fukushima Y, Miyatake S, Mizuguchi T, Saitsu H, Miyake N, Matsumoto N.	Clinical correlations of mutations affecting six components of the SWI/SNF complex: detailed description of 21 patients and a review of the literature.	<i>Am J Med Genet A</i>	In press		2013

Kaname T, Yanagi K, Naritomi K.	A commentary on the diagnostic utility of exome sequencing in Joubert syndrome and related disorders.	<i>J Hum Genet</i>	58(2)	57	2013
Jinam T, Nishida N, Hirai M, Kawamura S, Oota H, Umetsu K, Kimura R, Ohashi J, Tajima A, Yamamoto T, Tanabe H, Mano S, Suto Y, Kaname T, Naritomi K, Yanagi K, Niikawa N, Omoto K, Tokunaga K, Saitou N.	The history of human populations in the Japanese Archipelago inferred from genomewide SNP data with a special reference to the Ainu and the Ryukyuan populations.	<i>J Hum Genet</i> , 57: 787-795, 2012.	57(12)	787-795	2012
Yanagi K, Kaname T, Wakui K, Hashimoto O, Fukushima Y, Naritomi K.	Identification of four novel synonymous substitutions in the X-linked genes neuroligin 3 and neuroligin 4X in Japanese patients with autistic spectrum disorder.	<i>Autism Res Treat</i>	2012	724072	2012
Cheung W, Kotzamanis G, Abdulrazzak H, Goussard S, Kaname T, Kotsinas A, Gorgoulis VG, Grillot-Courvalin C, Huxley C.	Bacterial delivery of large intact genomic-DNA-containing BACs into mammalian cells.	<i>Bioeng Bugs</i>	3(2)	86-92	2012
He Y, Wang WR, Xu S, Jin L; Pan-Asia SNP Consortium.	Paleolithic Contingent in Modern Japanese: Estimation and Inference using Genome-wide Data.	<i>Sci Rep</i>	2	355	2012

Tsurusaki Y, Okamoto N, Ohashi H, Kosho T, Imai Y, Hibi-Ko Y, Kaname T, Naritomi K, Kawame H, Wakui K, Fukushima Y, Homma T, Kato M, Hiraki Y, Yamagata T, Yano S, Mizuno S, Sakazume S, Ishii T, Nagai T, Shiina M, Ogata K, Ohta T, Niikawa N, Miyatake S, Okada I, Mizuguchi T, Doi H, Saitsu H, Miyake N, Matsumoto N.	Mutations affecting components of the SWI/SNF complex cause Coffin-Siris syndrome.	<i>Nat Genet</i>	44(4)	376-378	2012
Migita K, Uehara R, Nakamura Y, Yasunami M, Tsuchiya-Suzuki A, Yazaki M, Nakamura A, Masumoto J, Yachie A, Furukawa H, Ishibashi H, Ida H, Yamazaki K, Kawakami A, Agematsu K.	Familial Mediterranean Fever in Japan.	<i>Medicine (Baltimore)</i>	91(6)	337-343	2012
Migita K, Ida H, Moriuchi H, Agematsu K.	Clinical relevance of MEFV gene mutations in Japanese patients with unexplained fever.	<i>J Rheumatol</i>	39(4)	875-877	2012
Higashimoto K, Nakabayashi K, Yatsuki H, Yoshinaga H, Jozaki K, Okada J, Watanabe Y, Aoki A, Shiozaki A, Saito S, Koide K, Mukai T, Hata K, Soejima H.	Aberrant methylation of H19-DMR acquired after implantation was dissimilar in soma versus placenta of patients with Beckwith-Wiedemann syndrome.	<i>Am J Med Genet A.</i>	158A(7)	1670-1675	2012

Ihara K, Yoshino M, Hoshina T, Harada N, Kojima-Ishii K, Makimura M, Hasegawa Y, Watanabe Y, Yamaguchi S, Hara T.	Coagulopathy in Patients With Late-Onset Ornithine Transcarbamylase Deficiency in Remission State: A Previously Unrecognized Complication.	<i>Pediatrics</i>	131(1)	e327-330	2013
Higashimoto K, Maeda T, Okada J, Ohtsuka Y, Sasaki K, Hirose A, Nomiyama M, Takayanagi T, Fukuzawa R, Yatsuki H, Koide K, Nishioka K, Joh K, Watanabe Y, Yoshiura K, Soejima H.	Homozygous deletion of <i>DIS3L2</i> exon 9 due to non-allelic homologous recombination between LINE-1s in a Japanese patient with Perlman syndrome.	<i>European Journal of Human Genetics</i>	In press		2013
Miyake N, Yano S, Sakai C, Hatakeyama H, Matsushima Y, Shiina M, Watanabe Y, Bartley J, Abdenur JE, Wang RY, Chang R, Tsurusaki Y, Doi H, Nakashima M, Saitsu H, Ogata K, Goto YI, Matsumoto N.	Mitochondrial Complex III Deficiency Caused by a Homozygous UQCRC2 Mutation Presenting with Neonatal-Onset Recurrent Metabolic Decompensation.	<i>Hum Mutat</i>	34(3)	446-452	2013
Ikewaki N, Sonoda T, Nakamura M, Ishizuki T, Higuchi G, Sugimoto S.	Action of <i>Taimatsu</i> fermented rice germ solution of human immune responses.	<i>J. of Kyushu Univ. of Health and Welfare</i>	14	177-182	2013
井田弘明, 有馬和彦, 金澤伸雄, 吉浦孝一郎	中條-西村症候群の原因遺伝子とプロテアソーム機能異常	リウマチ科 (科学評論社)	47(6)	654-660	2012
井田弘明, 有馬和彦, 金澤伸雄, 吉浦孝一郎	プロテアソーム病	炎症と免疫 (先端医学社)	20(6)	609-614	2012

井田弘明, 福田孝昭	自己炎症症候群の定義と分類	九州リウマチ	32(2)	75-78	2012
井田弘明, 福田孝昭	自己炎症症候群	日本臨床	70(suppl 8)	561-568,	2012
井田弘明	自己炎症症候群	日本医事新報	4615	78-83	2012

IV. おもな研究成果の刊行物・別冊

Identification of the First ATRIP-Deficient Patient and Novel Mutations in ATR Define a Clinical Spectrum for ATR-ATRIP Seckel Syndrome

Tomoo Ogi^{1,2,3*}, Sarah Walker^{3,4}, Tom Stiff³, Emma Hobson⁴, Siripan Limsirichaikul^{2,5}, Gillian Carpenter⁵, Katrina Prescott⁴, Mohnish Suri⁶, Philip J. Byrd⁷, Michiko Matsuse², Norisato Mitsutake^{1,2}, Yuka Nakazawa^{1,2}, Pradeep Vasudevan⁸, Margaret Barrow⁸, Grant S. Stewart⁷, A. Malcolm R. Taylor^{7*}, Mark O'Driscoll^{5*}, Penny A. Jeggo^{3*}

1 Nagasaki University Research Centre for Genomic Instability and Carcinogenesis (NRGIC), Nagasaki University, Sakamoto, Nagasaki, Japan, **2** Department of Molecular Medicine, Atomic Bomb Disease Institute, Nagasaki University, Sakamoto, Nagasaki, Japan, **3** Double Strand Break Repair Laboratory, Genome Damage and Stability Centre, University of Sussex, Brighton, United Kingdom, **4** Department of Clinical Genetics, Chapel Allerton Hospital, Leeds, United Kingdom, **5** Human DNA Damage Response Disorders Group, Genome Damage and Stability Centre, University of Sussex, Brighton, United Kingdom, **6** Clinical Genetic Service, City Hospital, Nottingham, United Kingdom, **7** School of Cancer Sciences, College of Medical and Dental Sciences, University of Birmingham, Birmingham, United Kingdom, **8** University Hospitals of Leicester NHS Trust, Leicester Royal Infirmary, Leicester, United Kingdom

Abstract

A homozygous mutational change in the *Ataxia-Telangiectasia and RAD3 related (ATR)* gene was previously reported in two related families displaying Seckel Syndrome (SS). Here, we provide the first identification of a Seckel Syndrome patient with mutations in *ATRIP*, the gene encoding ATR-Interacting Protein (ATRIP), the partner protein of ATR required for ATR stability and recruitment to the site of DNA damage. The patient has compound heterozygous mutations in *ATRIP* resulting in reduced ATRIP and ATR expression. A nonsense mutational change in one *ATRIP* allele results in a C-terminal truncated protein, which impairs ATR-ATRIP interaction; the other allele is abnormally spliced. We additionally describe two further unrelated patients native to the UK with the same novel, heterozygous mutations in *ATR*, which cause dramatically reduced ATR expression. All patient-derived cells showed defective DNA damage responses that can be attributed to impaired ATR-ATRIP function. Seckel Syndrome is characterised by microcephaly and growth delay, features also displayed by several related disorders including Majewski (microcephalic) osteodysplastic primordial dwarfism (MOPD) type II and Meier-Gorlin Syndrome (MGS). The identification of an ATRIP-deficient patient provides a novel genetic defect for Seckel Syndrome. Coupled with the identification of further ATR-deficient patients, our findings allow a spectrum of clinical features that can be ascribed to the ATR-ATRIP deficient sub-class of Seckel Syndrome. ATR-ATRIP patients are characterised by extremely severe microcephaly and growth delay, microtia (small ears), micrognathia (small and receding chin), and dental crowding. While aberrant bone development was mild in the original ATR-SS patient, some of the patients described here display skeletal abnormalities including, in one patient, small patellae, a feature characteristically observed in Meier-Gorlin Syndrome. Collectively, our analysis exposes an overlapping clinical manifestation between the disorders but allows an expanded spectrum of clinical features for ATR-ATRIP Seckel Syndrome to be defined.

Citation: Ogi T, Walker S, Stiff T, Hobson E, Limsirichaikul S, et al. (2012) Identification of the First ATRIP-Deficient Patient and Novel Mutations in ATR Define a Clinical Spectrum for ATR-ATRIP Seckel Syndrome. *PLoS Genet* 8(11): e1002945. doi:10.1371/journal.pgen.1002945

Editor: Andrew O. M. Wilkie, University of Oxford, United Kingdom

Received: April 25, 2012; **Accepted:** July 26, 2012; **Published:** November 8, 2012

Copyright: © 2012 Ogi et al. This is an open-access article distributed under the terms of the Creative Commons Attribution License, which permits unrestricted use, distribution, and reproduction in any medium, provided the original author and source are credited.

Funding: This work has been supported by Special Coordination Funds for Promoting Science and Technology from the Japan Science and Technology Agency (JST) to TO and YN; a Global COE Program from the Ministry of Education, Culture, Sports, Sciences, and Technology of Japan to TO, MM, NM, SL, and YN; and by a Grant in Aid for Scientific Research KAKENHI (24681008) from the Japan Society for the Promotion of Science, a science research grant from Inamori Foundation, a medical research grant from Mochida Memorial Funds for Medical and Pharmaceutical Research, a medical research grant from Daiichi-Sankyo Foundation of Life Science, and a medical research grant from Takeda Science Foundation to TO. The PAJ laboratory is supported by the Medical Research Council, the Association for International Cancer Research, and the Wellcome Research Trust. The MO laboratory is supported by Cancer Research UK, Medical Research Council, and Leukaemia Lymphoma Research. MO and GSS are CR-UK Senior Cancer Research Fellows. The funders had no role in study design, data collection and analysis, decision to publish, or preparation of the manuscript.

Competing Interests: The authors have declared that no competing interests exist.

* E-mail: m.o-driscoll@sussex.ac.uk (MO); A.M.R.Taylor@bham.ac.uk (AMRT); p.a.jeggo@sussex.ac.uk (PAJ); togi@nagasaki-u.ac.jp (TO)

† Current address: Faculty of Pharmacy, Silpakorn University, Nakhon Pathom, Thailand

‡ These authors contributed equally to this work.

Introduction

Seckel Syndrome (SS) (OMIM 216000) is an autosomal recessive disorder characterised by marked microcephaly, intra-uterine and post-natal growth retardation, developmental delay

and characteristic facial features, encompassing micrognathia (small and receding chin), receding forehead and pronounced nose [1]. Majewski (microcephalic) osteodysplastic primordial dwarfism (MOPD) type II and Meier-Gorlin Syndrome (MGS) also display microcephaly and primordial dwarfism [2,3]. How-

Author Summary

Seckel Syndrome (SS) is a rare human disorder characterised by small head circumference and delayed growth. Patients can show additional features including abnormal bone development, receding chins, sloping foreheads, and small ears. In 2003, we identified *ataxia telangiectasia and Rad3 related (ATR)* as a causal genetic defect in two related families displaying SS. However, additional patients with mutations in *ATR* have not hitherto been identified. Here, we describe two further patients with novel mutations in *ATR*. Additionally, we identify a patient with mutations in *ATRIP*, which encodes an interacting partner of *ATR*, representing a novel genetic defect causing SS. *ATR* functions to promote the ability of cells to recover from difficulties encountered during replication. We show that patient-derived cells have reduced *ATR* and *ATRIP* protein levels and defective *ATR/ATRIP* function. Our identification of further *ATR-ATRIP* defective patients and a consideration of their clinical features aids the characterisation and identification of this form of SS and provides insight into the role played by the *ATR-ATRIP* complex during development.

ever, each of these disorders display an additional spectrum of features conferring clinical distinction. Despite this, on an individual basis, assigning patients to a specific classification is difficult. Additionally, primary microcephaly represents a disorder displaying pronounced microcephaly without marked impact on growth [4]. Five loci conferring SS have been described with four genes identified [5,6]. The first causal genetic defect identified for SS was the *Ataxia-Telangiectasia and RAD3 related (ATR)* gene [7]. A homozygous mutation in *ATR* was identified in two related SS families and cell-based studies provided strong evidence for an impact on *ATR* function in patient cell lines. This sub-class of SS was designated *ATR-SS*. More recently, mutations in *CTIP* were identified in a SS patient as well as in a family described as displaying Jawad Syndrome [8]. Additionally, mutations in *CENPJ* and *CEP152*, two centrosomal proteins, have been described in SS patients, although mutations in these genes more frequently confer primary microcephaly [9,10]. Mutations in *PCNT*, which encodes a centrosomal protein, and *ORC1L*, a component of the original licensing complex, were reported in patients originally classified as SS although in both cases retrospective analysis revealed that such mutations more frequently cause MOPD type II or MGS, respectively, highlighting the diagnostic challenge faced in the clinic [11–15]. These studies demonstrate that evaluation of multiple patients is required to provide insight into the spectrum of clinical features conferred by specific gene defects, which ultimately aids an understanding of the role of the defective protein during development. To date all *ATR-SS* patients belong to one of two related families, which harbour the identical homozygous mutation in *ATR*, thereby limiting the characterisation of the clinical phenotype conferred by *ATR* deficiency. Furthermore, no patients deficient in *ATR* interacting protein, *ATRIP*, which is required for *ATR* stability, have hitherto been described.

ATR, like the related Ataxia-Telangiectasia mutated (*ATM*) protein, is a phosphoinositol-3 kinase (*PI3*)-like kinase that functions at the centre of a signal transduction network activated by DNA damage, and most importantly, by replication fork stalling [16]. *ATR* and *ATM* share phosphorylation targets but whilst *ATM* is activated by DNA double strand breaks (*DSBs*) that arise, for example, following exposure to ionising radiation (*IR*),

ATR is activated by single stranded (*ss*) regions of DNA that arise following replication fork stalling or exposure to agents that induce bulky DNA adducts [17,18]. Importantly, since replication fork stalling occurs during most cycles of replication, *ATR* is essential. *ATM*, in contrast, is non-essential presumably because endogenous *DSBs* arise infrequently. *ATR* forms a stable complex with *ATR-interacting protein (ATRIP)*, which is required for *ATR* stability [19]. Further, *ATRIP* is required for *ATR* localisation to *ssDNA* regions and hence for *ATR* activation. Consequently, in a range of organisms loss of *ATRIP* or its homologue, phenocopies *ATR* deficiency [17,20–22]. Although *ATM* and *ATR* share overlapping substrates, *ATR* specifically phosphorylates *Chk1* whilst *ATM* phosphorylates the related kinase, *Chk2*. The major functions of *ATR* are to activate cell cycle checkpoint arrest, stabilise stalled replication forks and promote replication fork restart, which is achieved through its ability to phosphorylate a range of substrates including *p53* and *H2AX* [18,23,24]. Interestingly, in the context of SS, *CtIP* promotes DNA end resection, which leads to *ssDNA* formation, the lesion activating *ATR*. Hence, *CtIP* functions in a mechanism leading to *ATR* activation. It is noteworthy that cells derived from *PCNT*-mutated MOPD type II patients are also defective in *ATR*-dependent G2/M checkpoint arrest although upstream steps in the *ATR*-signalling pathway are activated normally [11]. These findings suggest that *PCNT* is required for an important end-point of *ATR* function. Additionally, the origin licensing complex, components of which are mutated in MGS, is required for the initiation of replication and *ORC1L*-deficient MGS cell lines display slow S phase progression [13]. Similarly, *ATR* promotes S phase progression by facilitating recovery from replication fork stalling. Together, these findings demonstrate mechanistic overlap between *ATR*, *PCNT* and *ORC1L*, which may underlie some clinical overlap in the disorders conferred by mutations in the genes encoding these proteins.

Here, we provide the first description of a SS patient with mutations in *ATRIP*. Interestingly, the mutational change in one *ATRIP* allele causes impaired *ATR-ATRIP* interaction and our extensive cellular analysis confirms a deficiency in *ATR* signalling and damage responses. Additionally, we describe two further, unrelated patients with mutations in *ATR*. The identification and clinical description of an *ATRIP* patient and two further *ATR* patients provides a more definitive characterisation of the clinical phenotype conferred by *ATR* deficiency.

Results

Cells derived from patient CV1720 display a compromised DNA damage response

Patient CV1720 displayed severe microcephaly, growth delay and dysmorphic facial features and was classified as a SS patient (see Table 1 and Figure S1A for details of the clinical features). Cell line CV1720 is a lymphoblastoid cell line (*LBL*) derived from the patient; fibroblasts were not available. Cells from the previously described *ATR-SS* (*DK0064*) patient display impaired DNA damage responses and phosphorylation of *ATR* substrates [7]. To determine whether CV1720 cells are defective in *ATR*-dependent G2/M checkpoint arrest, the mitotic index (*MI*) was monitored at 2 h following UV exposure, a form of DNA damage known to activate *ATR*-dependent checkpoint arrest. Whilst *WT LBLs* show a significantly reduced *MI* following UV exposure compared to undamaged cells, CV1720 cells showed only a modest decrease similar to that observed in *DK0064 (ATR-SS)* cells (Figure 1A). Cells from the parents of patient CV1720

Table 1. Clinical features of ATR/ATRIP-deficient patients.

	ATRIP-SS		ATR-SS	27-4BI	19-8BI
Ethnicity	Gujarati-Indian (consanguineous)		Pakistani (consanguineous)	English	English
Birth.					
OFC (cm)	27.1		24 (-8SD)	27	24.2
Wgt (Kg)	2.06		1.1 (-3SD)	1.15	0.77
Hgt (cm)	NR		NR	36	NR
Age.					
	14 mts	3 yrs 3 mts	9 yrs	20 mts	4.5 yrs
OFC (cm)	-9SD	-10SD	-12SD	-10SD	-10SD
Wgt (Kg)	-5SD	-6SD	-3.3SD	-8SD	-7SD
Hgt (cm)	-5SD	-6.5SD	NR	-8SD	-8SD
Face	Micrognathia, receding forehead, prominent nose.		Micrognathia, receding forehead, prominent nose.	Micrognathia, prominent nose, hypoplastic alae nasi, low set columella, deep set short palpebral fissures.	Micrognathia, blepharophimosis, short palpebral fissures. Prominent nose; high nasal bridge. High anterior hairline.
Teeth	Dental crowding.		Dental crowding and malocclusion.	4 teeth at 20 months.	Dental crowding.
Ears	Small lobes.		Posteriorly rotated with absent lobes.	Small, round, low set with poorly formed antihelix tragus & antitragus. Absent lobes.	Small ears with absent lobes
Hands	Bilateral 5 th finger clinodactyly.		Multiple ivory epiphysis.	Small, tapering fingers.	Bilateral 5 th finger clinodactyly. 5 th metacarpels appear short. Blue colouration to both thenar eminence.
Skeletal Survey	Delayed bone age (wrist & hips), symmetric dwarfism.		Microcrania with fuse sutures. Mild thoracic kyphosis. Ribs angulated posteriorly. Narrow iliac blades, cox valga and minor subluxation of the hips. No dislocation of the radial heads	Symmetric dwarfism. Small patellae. No joint hypermobility or kyphoscoliosis.	Symmetric dwarfism. Copper beaten skull. No ossification of the patellae (age 4 yrs). Marked hip & shoulder flexibility. No kyphosis.
Endo-crinology	Normal IGF1, TFT, LH, FSH & cortisol.		NA	NA	NA
MRI	14 mts: generalised cerebral atrophy, normal ventricular systems. Delayed myelination in the anterior limb of the internal capsule. Pituitary is present though of unusual shape with absent fossa.		NA	NA	2 yrs: abnormal gyration in posterior aspect of the cingulate gyrus extending into the parietal occipital region. Hypoplastic corpus collasum.
Other	NR		Developmental delay. Walked at 7 yrs.	No abnormal skin pigmentation. Small feet with metatarsus adductus	No abnormal skin pigmentation. Developmental delay. Sat at 15 mts, walked at 3 yrs 10 mts. High pitched voice, asthma, multiple chest infections, feeding difficulties-reflux (gastrostomy fed). Multiple liver cysts consistent with Caroli's disease found at 17 mts.

NR; not recorded. NA; not assessed.
doi:10.1371/journal.pgen.1002945.t001

(CV1780 and CV1783) displayed normal G2/M checkpoint arrest.

We have previously observed that cells from other SS patients display defects in ATR-dependent G2/M checkpoint arrest but activate upstream steps in the ATR signalling cascade normally [25]. This is exemplified by cell lines from MOPD type II patients with mutations in *PCNT*, which are defective in ATR-dependent G2/M checkpoint arrest but proficient in ATR phosphorylation events [11]. Therefore, next, we examined whether CV1720 LBLs efficiently activate upstream steps in ATR signalling. Since these assays predominantly reflect the response of replicating phase cells, we first verified that CV1720 and control LBLs harbour a similar percentage of S phase cells (Figure S2). Pan-nuclear phosphorylation of H2AX (γ H2AX) after replication fork stalling represents

an ATR-specific damage response [24]. Strikingly, whilst exposure to 5 mM HU for 2 h resulted in an elevated number of cells staining positively for γ H2AX in WT cells, this was not observed in either CV1720 or DK0064 (ATR-SS) cells (Figure 1B). We note that although previous studies have shown that ATM can be activated and phosphorylate γ H2AX at DSBs arising following HU treatment in the absence of ATR due to enhanced fork collapse, this was not observed at 2 h post 5 mM HU exposure in these patient cells most likely due to residual ATR activity and/or the early times examined [26,27]. Chk1 represents an important ATR substrate required for G2/M checkpoint arrest. To examine Chk1 activation, we carried out Western Blotting using p-Chk1 antibodies. Following the same UV exposure conditions (2 h post 5 Jm⁻²) employed to examine G2/M checkpoint arrest, we

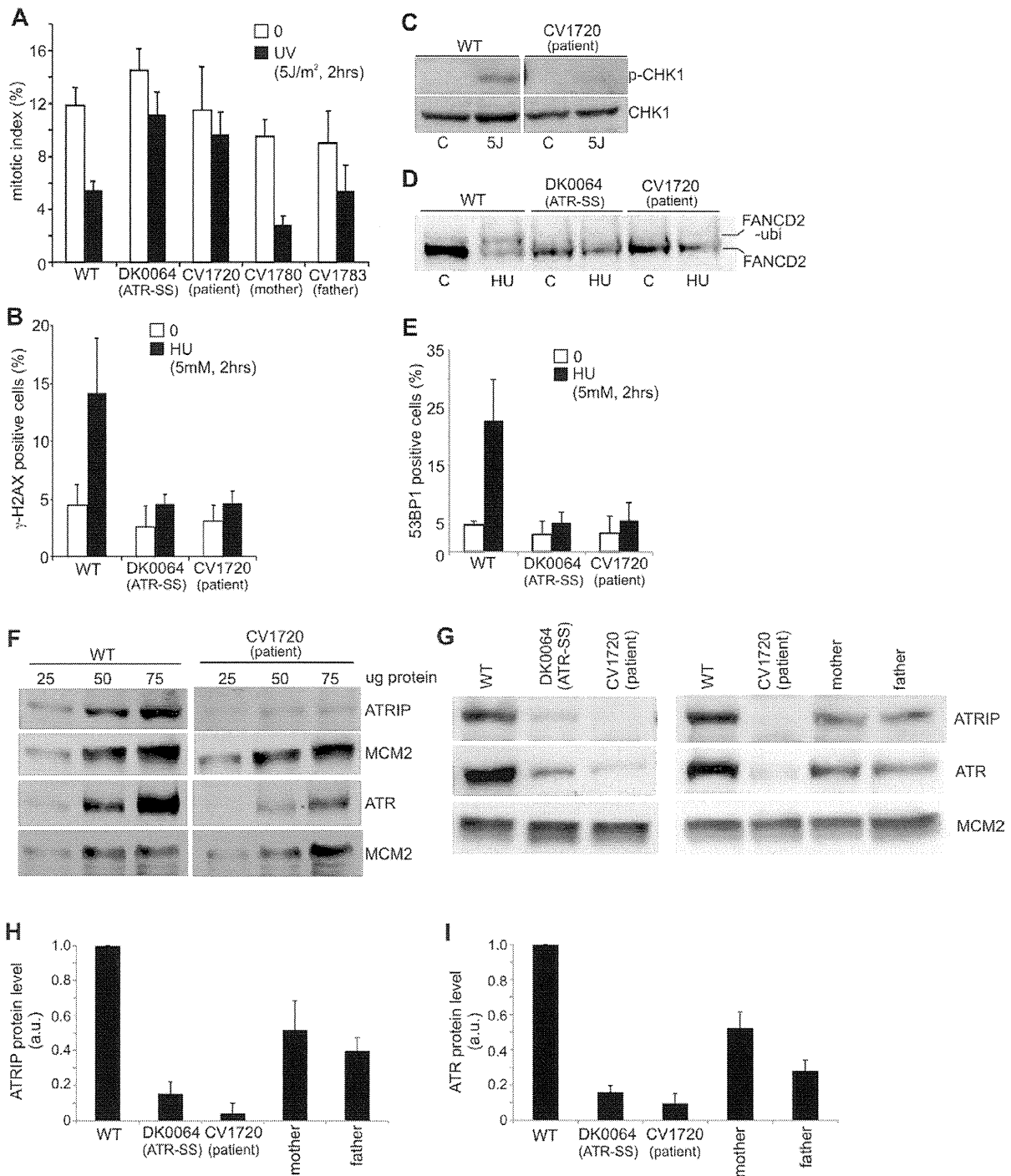


Figure 1. CV1720 cells show impaired ATR-dependent DNA damage responses. A) WT, DK0064 (ATR-SS), CV1720 (patient), CV1780 (patient's mother) and CV1783 (patient's father) cells were exposed to 5 Jm^{-2} UV and the mitotic index (MI) assessed 2 h post exposure. A greater than two fold decrease in mitotic index is observed in WT and both paternal cell lines but not in DK0064 (ATR-SS) or CV1720 (patient) cells. B) Cells were exposed to 5 mM HU for 2 h and the percentage of p-H2AX (γ -H2AX) positive cells assessed by immunofluorescence. Note that HU causes pan nuclear p-H2AX formation rather than defined foci as observed after exposure to ionising radiation. Thus, the percentage of γ -H2AX positive cells was scored. C) Cells were exposed to UV (5 Jm^{-2}) and subjected to Western Blotting (WB) using p-Chk1 (p-Ser317) antibodies at 2 h. Chk1 expression was shown to be similar in WT and patient cells (lower panel). D) Cells were exposed to 3 mM HU for 2 h and whole cell extracts analysed by WB using FANCD2 antibodies. The ubiquitylation of FANCD2, detectable by a product with reduced mobility, is diminished in DK0064 (ATR-SS) and CV1720 cells compared to WT cells. E) Cells were exposed to 5 mM HU and examined for the percentage of cells showing >5 53BP1 foci at 2 h post exposure. 53BP1 foci formation is reduced in DK0064 (ATR-SS) and CV1720 cells compared to WT cells. F–I) The indicated cells were processed by WB using

ATRIP or ATR antibodies. MCM2 was used as a loading control. F shows the analysis of a range of protein levels for accurate comparison. CV1720 (patient) cells show markedly reduced ATR and ATRIP protein levels. G shows that both parental lines have approximately half the level of ATR and ATRIP compared to two WT cell lines. DK0064 (ATR-SS) and CV1720 cells, in contrast, have more dramatically reduced ATR and ATRIP protein levels. 50 μ g protein was loaded. WT in all panels was GM2188. Patient, mother and father were as shown in panel A. H and I show the quantification of ATRIP and ATR protein levels from at least three independent WB experiments.
doi:10.1371/journal.pgen.1002945.g001

observed a pronounced p-Chk1 band in WT LBLs but not in CV1720 cells although Chk1 levels were similar in the two lines (Figure 1C). These results provide strong evidence that CV1720 show impaired ATR-dependent substrate phosphorylation.

A further ATR-dependent response is mono-ubiquitylation of FANCD2 following exposure to HU [28]. Mono-ubiquitylated FANCD2 can be detected by the presence of a slowly migrating isoform of FANCD2 generated post exposure to 3 mM HU. Whilst such a product was detected in WT cell extracts, it was absent in CV1720 and DK0064 (ATR-SS) cell extracts (Figure 1D). Finally, ATR also regulates the formation of 53BP1 foci following replication fork stalling via a Chk1-dependent process. We observed a failure to form 53BP1 foci following exposure to 5 mM HU in CV1720 and DK0064 (ATR-SS) LBLs in contrast to WT LBLs (Figure 1E), consistent with the diminished levels of p-Chk1 observed in CV1720 cells.

Collectively, these studies provide strong evidence that CV1720 cells are defective in an upstream step of the ATR-dependent signalling response defining them as distinct to the majority of previously characterised SS cell lines, which, though defective in UV-induced G2/M checkpoint arrest, are proficient in upstream steps of the ATR signalling response [25].

Reduced ATR and ATRIP protein expression in CV1720 cells

Given the overlapping cellular phenotype between CV1720 and DK0064 (ATR-SS) cells, we examined CV1720 cells for expression of ATR and ATRIP protein by Western Blotting. Strikingly, we observed markedly reduced levels of both ATR and ATRIP in CV1720 cells (Figure 1F). Since ATRIP stabilises ATR, this does not distinguish whether the primary defect lies in ATR or ATRIP and indeed a similar reduced level of ATR and ATRIP was observed in DK0064 (ATR-SS) cells (Figure 1G). Significantly, we observed reduced ATRIP and ATR in both parental LBLs (CV1780 and CV1783), which was approximately 50% of the level in WT LBLs (Figure 1G–I).

Sequencing analysis reveals mutational changes in ATRIP in CV1720 cells

To examine whether the causal genetic defect in CV1720 lies in *ATR* or *ATRIP*, we carried out sequencing of the two genes. First, we undertook PCR-based gDNA sequencing of the 47 exons and neighbouring exon-intron boundaries of the human *ATR* gene from CV1720 cells and failed to observe any mutational changes likely to be of functional significance. Next, we undertook gDNA sequencing of *ATRIP* exons and observed a heterozygous mutational change, c.2278C>T, in exon12 which generated a stop codon predicting a truncated protein at position arginine 760 (p.Arg760*) (Figure S3). However, no mutational changes in any other exons were identified although we detected several novel intronic changes that could potentially impact on splicing (Table S1). Significantly, the c.2278C>T mutational change was observed as a heterozygous change in the patient's mother but not in the father (Figure S3).

We also performed RT-PCR sequencing of *ATRIP* cDNA from CV1720 and both parents. These analyses revealed a low level of a

smear PCR product following amplification of the 5' *ATRIP* cDNA region using patient but not control cDNA (data not shown). Following multiple analyses, we found specifically that RT-PCR amplification using primers located in exons 1 and 4, reproducibly yielded a smeared product from CV1720 cDNA with discrete bands at 458 bp (the expected product size) and 325 bp whereas only the 458 bp product was observed using cDNA from WT cells (Figure 2A). Direct sequencing of the gel purified smaller (325 bp) and full-length (458 bp) RT-PCR products showed that the small fragment specifically lacked exon 2. Sequencing analysis of the RT-PCR product of CV1720 cDNA using the same primers revealed the predicted double sequence with the product lacking exon 2 being less than 50% of the product containing exon 2 (Figure 2B). It is notable that there were also some PCR products larger than the full length product although a discrete band was not evident. In sequencing the RT-PCR product, we observed some that harboured intron 2 sequences although these represented a minor product relative to that lacking exon 2. Collectively, these findings strongly suggested that there could be mis-splicing in CV1720 cells with loss of exon 2 being the major product.

To assess this further, qRT-PCR was undertaken using sets of primers that allow selective amplification of the WT and mutant products (c.2278C>T mutant as well as the mis-spliced product). The aim was to determine if the mis-spliced product originated from the paternal allele and if it impacted upon the transcript level. Primer pairs, P1 and P3C, located in exons 12 and 13, respectively, allow selective amplification of the WT (paternal) c.2278C allele whilst primers P2 and P3C selectively amplify the mutated (maternal) c. 2278C>T allele (Figure 2C). As expected, the mutant (c.2278C>T)-allele-specific PCR product (right columns, red bars) was only detected in the patient and mother whereas the WT-specific PCR product (left columns, blue bars) was detected in all samples, demonstrating that the primers distinguished the two alleles (Figure 2C). The results also showed that the c.2278C>T and the WT (c.2278C) alleles were expressed at nearly equal levels (normalised against *HPRT1*) in the mother (compare blue and red bars labelled 'mother' in Figure 2C), suggesting that the c.2278C>T *ATRIP* mRNA is not subject to nonsense mediated RNA decay (NMD) (Figure 2C).

To evaluate the expression level of the mis-spliced *ATRIP* mRNA, we designed primers located at the exon 2/exon 3 boundary (primer P4) and within exon 3 (primer 6C) to allow selective amplification of the correctly spliced mRNA (Figure 2D); primers located at the exon 1/exon 3 boundary (primer P5) and within exon 3 (primer 6C) selectively amplify the mis-spliced mRNA. Whilst the correctly spliced product was amplified to similar (although slightly different) extents from father, mother and patient mRNA (compare the column heights, left panel in Figure 2D), the mis-spliced product was more abundant in the patient and father, suggesting that mis-splicing is a consequence of a mutational change linked to the paternal allele (compare the column heights, right panel in Figure 2D). Since we observed nearly equal expression levels of the wild type (c.2278C) and mutant (c.2278C>T) alleles in the mother (Figure 2C, compare the right and left panels), we considered that the PCR products derived from the mother using primers P4/P6C or P5/P6C would

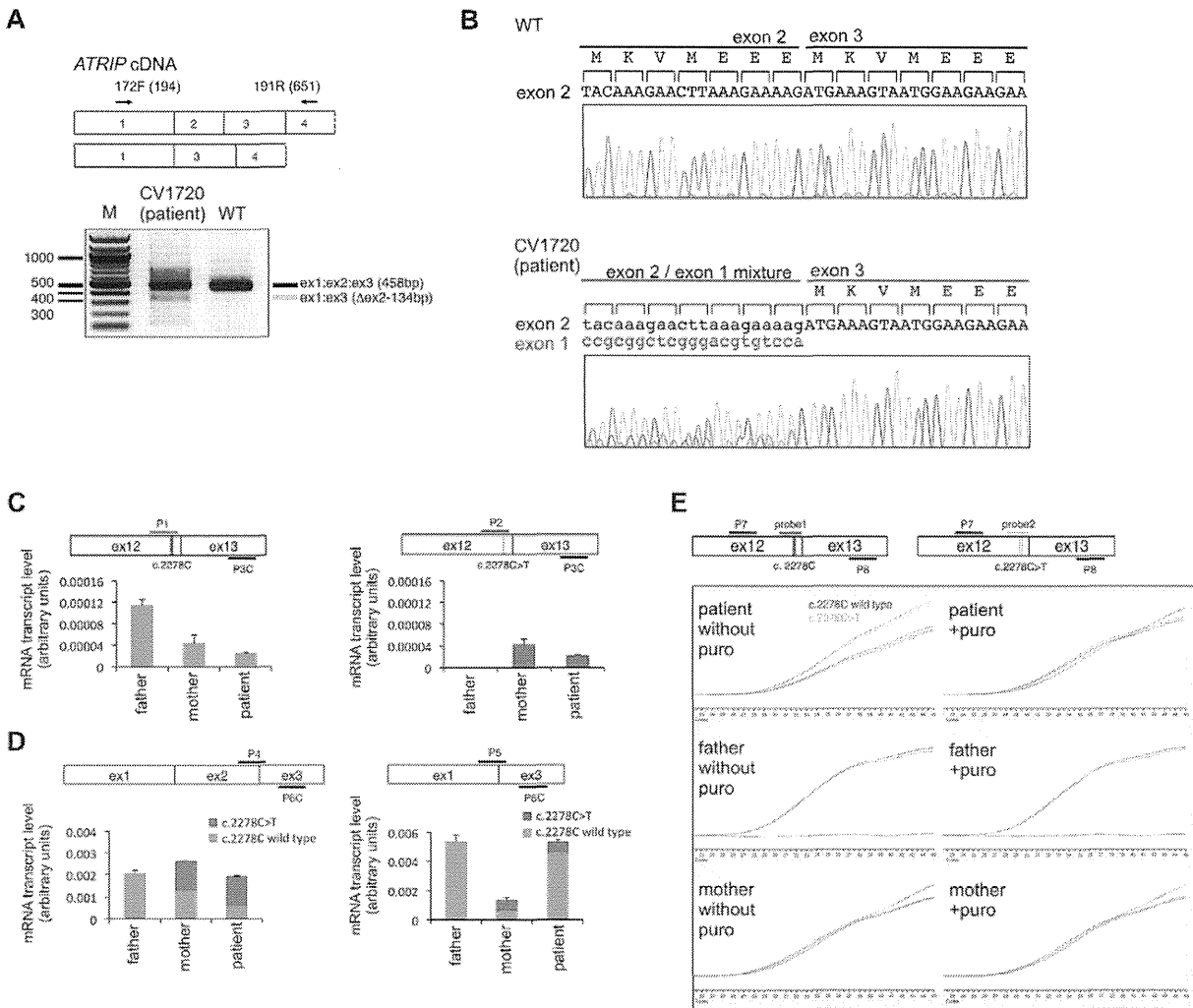


Figure 2. Identification of mutational changes in *ATRIP* in CV1720. A) Upper panel shows primer pairs used to distinguish cDNA products encompassing or lacking exon 2. Lower panel shows RT-PCR products obtained using the primers shown in the upper panel. RT-PCR from patient CV1720 generated a smeared product with a defined band of 458 bp, as observed in WT cells, and a weaker band of 325 bp. The latter band was not detected using cDNA from WT cells (MRC5). A similar single 458 bp band was obtained using the same primers with cDNA derived from a distinct wild type cell line (GM2188; data not shown). (B) Sequencing of the RT-PCR products derived from WT (MRC5) and patient (CV1720) cells. A double sequence pattern at the exon 2–3 boundary is observed using patient CV1720 cDNA. (C) Selective quantitative amplification of the WT or 2278C>T *ATRIP* alleles. Primers located in *ATRIP* exon 12 and 13 were designed to selectively amplify the WT (c.2278C) (P1 and P3C) versus the mutated (c.2278C>T) (P2 and P3C) alleles. The WT PCR product is shown in blue and the c.2278C>T PCR product in red. The exon 12 mutated allele is only observed in the patient and mother cDNA whilst the WT allele is observed in the patient, mother and father cDNA although the level is reduced in the patient and mother. (D) qRT-PCR analysis of *ATRIP* splicing variants from patient CV1720 and parental cells. qRT-PCR analysis of the level of the normally spliced (encompassing exons 1–2–3) and the aberrantly spliced (Δ exon2) *ATRIP* cDNA in the patient and parent cells. PCR primers were designed at the exon2-exon3 or exon1-exon3 boundaries to selectively amplify the splicing variants. Transcripts from *HPRT1* were used as a quantification control. The correctly spliced transcript from the paternal allele of the patient (wild type c.2278C, blue fraction in the cumulative bar labelled, 'patient', at the left panel) was estimated to be ~25% of the normal level. (E) The mis-spliced paternal allele is subject to nonsense mediated mRNA decay (NMD). Cycleave-qPCR confirmed that the *ATRIP* c.2278C>T mutant allele was expressed exclusively in the patient and the mother. The *ATRIP* exon12-13 fragment was amplified with PCR primers P7/P8 as shown in the figure. A set of fluorescent probes were used to distinguish the WT versus c.2278C>T allele (probe1 and probe2, respectively). In the patient, the paternal mRNA transcript level (emerald lines) is low because of NMD (top left). Puromycin treatment eliminated the NMD and the paternal transcript level returned to the normal level. In all panels WT represented MRC5, patient was CV1720 and parents were as shown in Figure 1A. doi:10.1371/journal.pgen.1002945.g002

be equally derived from the c.2278C and c.2278C>T alleles, which have, therefore, been depicted as equal sized contributions (shown in red or blue in mother columns in Figure 2D). Similarly, the mutant c.2278C>T allele is likely to be expressed at an equal level in the patient as in the mother (shown in red in patient

columns in Figure 2D). Based on these assumptions, we estimated that the normally spliced WT mRNA is reduced to around 1/4 of the WT level in the patient and to 3/4 in the father (shown in blue in the left hand panel in Figure 2D). Assuming that the c.2278C>T allele is fully inactivated (see below), the patient

therefore has around 25% of ATRIP activity compared to a normal individual.

The findings above suggested that the mis-spliced mRNA, which generates an out of frame cDNA, is subject to NMD. To examine this and substantiate our findings, qRT-PCR was also carried out using fluorescent cycleave probes with or without exposure to puromycin, an antibiotic which prevents NMD (Figure 2E) [29]. Primers (P7 and P8) and fluorescent probes (probe 1 and 2) were designed to allow amplification of a product encompassing exon 12–13 that distinguished the maternal (probe 2) from the paternal (probe 1) allele. We confirmed detection of the c.2278C>T allele exclusively in the patient and mother as well as the WT allele in all samples (Figure 2E). In the mother, the wild type (c.2278C) and mutant (c.2278C>T) signals were detected at equal levels regardless of whether puromycin was added, indicating that the alleles are equally expressed and are not subjected to NMD. In patient CV1720, the WT product was reduced relative to the mutant product in the absence of puromycin but was at similar levels in the presence of puromycin (Figure 2E). These findings are consistent with the notion that the mRNA expressed from the parental allele is aberrantly spliced and partially subject to NMD. Perhaps surprisingly, we did not detect any obvious difference of the WT product following puromycin treatment in the father; however, in this case, we anticipate a 25% decreased product, which is unlikely to be detected without an internal control. However, despite this, there was evidence for abnormal splicing in the paternal cDNA from analysis of the PCR products spanning exons 1–3 (Figure 2B, 2D).

Finally, to gain insight into the basis underlying mis-splicing, we sequenced introns 1 and 2 from the patient, mother, and father and identified a previously unreported mutational change in intron 2, 13 bp from the intron-exon 2 boundary in the patient and paternal gDNA (Table S1). However, given the modest impact on splicing we did not attempt to examine whether this represented the causal mutational change affecting splicing.

Arg760* ATRIP does not promote ATR-dependent G2/M arrest and reduces ATR-ATRIP interaction

It is likely that *ATRIP* c.2278C>T causes an impacting mutational change since the low levels of ATRIP protein (10–20% WT levels) in CV1720 cells suggest that p.R760* ATRIP is unstable (given that the mRNA level of this allele is normal). To substantiate that p.R760* expression impairs the ATR-dependent response to DNA damage, we examined whether its expression could complement the G2/M checkpoint defect of CV1720 cells. We also examined whether p.R760* might exert a dominant negative impact (since this represented a possible explanation for the low ATRIP protein level in CV1720 cells). The c.2278C>T mutational change was introduced into *ATRIP* cDNA by site directed mutagenesis. cDNA encoding WT *ATRIP* and/or R760* ATRIP was transiently transfected into LBLs and G2/M checkpoint arrest examined at 2 h post exposure to 5 Jm⁻² UV. Consistent with previous findings, WT but not CV1720 cells showed a G2/M checkpoint arrest (Figure 3A). Whilst transfection with WT *ATRIP* cDNA completely rescued the G2/M checkpoint defect of CV1720 cells, no correction was observed in CV1720 cells following expression of c.2278C>T *ATRIP* cDNA (encoding R760* ATRIP). Surprisingly, expression of WT *ATRIP* cDNA also corrected the G2/M checkpoint defect in DK0064 (ATR-SS) cells, which we propose could result from elevated ATRIP expression causing stabilisation of residual ATR protein, since ATR-SS cells have low ATR and ATRIP expression. Significantly, c.2278C>T *ATRIP* cDNA was unable to rescue ATR-SS cells.

Finally expression of c.2278C>T *ATRIP* cDNA in WT cells did not affect G2/M checkpoint arrest demonstrating that p.R760* ATRIP does not exert a dominant negative impact. Collectively, we conclude that p.R760* ATRIP impairs upon ATRIP function.

Next we examined how loss of the ATRIP C-terminus might impact upon ATRIP function. Two studies have previously observed that the C-terminal region of ATRIP is required for interaction with ATR [21,30]. Falck *et al* [30] reported that ATR-ATRIP interaction required the C-terminal 32 amino-acids of ATRIP (769–791) whilst Ball *et al* [21] found that interaction was abolished in a protein that lacked exon 11, which encompasses amino-acids 658–684. Arg760 lies close to these regions. To examine whether p.R760* ATRIP can interact with ATR, HA-tagged WT or c.2278C>T (*ATRIP* R760*) cDNA was co-expressed with untagged WT *ATR* cDNA in HEK293 cells. Following IP with HA-agarose, the level of co-immunoprecipitated ATR was assessed by Western Blotting. Although there was a low level of non-specific ATR binding to the HA beads, the level of ATR present after HA-R760* ATRIP expression (derived from c.2278C>T *ATRIP* cDNA) was substantially lower than after HA-WT ATRIP expression (Figure 3B left panel). Both WT and R760* ATRIP were efficiently expressed, however (Figure 3B right panel). Thus, we conclude that R760* impairs the binding of ATRIP to ATR.

Identification of further patients with mutations in *ATR*

In the course of our functional characterisation of cell lines from SS patients, we examined LBLs derived from two SS patients, 27-4BI and 19-8BI (see Figure 4A, Figure S4, and Table 1 for clinical details). Western Blotting revealed that both cell lines displayed substantially reduced ATR protein whilst showing normal expression of other DNA damage response components, including CtIP, TOPBP1 and RAD17 (Figure 4B). 27-4BI also had reduced ATRIP levels. Additionally, the 27-4BI cell line expressed normal levels of PCNT, excluding MOPD type II as a potential genetic diagnosis, since most of these patients exhibit severely reduced PCNT expression. These findings raised the possibility that the patients could harbour mutations affecting ATR or ATRIP expression. Sequencing of *ATR* cDNA revealed the same c.3477G>T mutational change in both patients (Figure S5A). This change causes an amino acid substitution, p.Met1159Ile, which lies within a conserved UME (NUC010) domain of ATR. UME domains, and particularly the methionine residue within the domain, are highly conserved in ATR species, including yeast although their function is unknown (Figure 4C and 4D).

The second *ATR* mutation identified was c.6897+464C>G;p.Val2300Gly fs75*, which, surprisingly, was also present in both patients. RT-PCR sequencing showed that a 142 bp sequence, which originated from a repeat region present in intron 40, was inserted at the boundary between exon 40 and 41 in both patients (Figure S5C). Genomic sequencing revealed the presence of a single C>G mutation in intron 40, which generates a preferred splice signal causing insertion of the intron sequence to the start of exon 41 (Figure S5D for further details). This insertion causes a frameshift and the generation of a stop codon at c.6978 in exon 41. Sequencing of *ATRIP* cDNA in patient 27-4BI failed to reveal any mutational changes. Thus, our findings provide strong evidence that mutational changes in ATR underlie the reduced ATR/ATRIP expression observed in both patients.

To verify that these mutational changes impact upon ATR function, we examined whether 27-4BI cells could activate UV-induced ATR-dependent G2/M checkpoint arrest. Significantly, we observed an inability to activate UV-induced G2/M checkpoint arrest in 27-4BI cells similar to that observed in DK0064